Introduction

The technological advances made in production types are rapidly changing the landscape in terms of manufacturing capabilities. One of these technologies is additive manufacturing or 3D printing. 3D printing techniques can also be used in aerospace applications such as prototyping, wind tunnel model manufacturing or UAV production. This thesis focuses on 3D printed material properties under different print conditions and their combination with different wing structures. The static structural analysis under certain flow parameters were done to assess the effect both material and structural differences cause.

Giriş

Üretim teknolojilerindeki gelişmeler imalat yöntemlerini hızla değiştirmeye başlamıştır. Bu teknolojilerden biri katmanlı üretim yada 3B yazmadır. Bu 3B yazma teknolojileri hava-uzay uygulamalarında da kullanım yerleri vardır örneğin; prototipleme, rüzgar tüneli modeli üretimi ve insansız hava aracı üretimi. Bu tez 3B yazılan malzemelerin, farklı basma parametreleri altında gösterdikleri özellikleri ve bunların farklı kanat yapılarıyla kombinasyonlarına odaklanır. Belli akış parametresi altında static yapısal analizler yapılmıştır ki hem malzeme hem de yapısal farklılıkların oluşturduğu etki gözlemlenebilsin.

3D printers have been around for a long time. However, they have seen a rise in widespread use all around the World in recent years. 3D printers are not only being used in industrial companies but have also entered many one's homes. The rise of 3D printer technology can be attributed to the steadily falling prices on 3D printers. The steady fall of cost is described…… ***"I think it's a combination of cheaper hardware, economies of scale, and figuring out where to cut corners on low-end printers," Mark Frauenfelder*** ***https://arstechnica.com/information-technology/2013/06/why-basic-3d-printers-are-crazy-cheap-now/*** …….

3D printers offer a great benefit as they make prototype production much easier than conventional methods. 3D printers make it both more affordable and faster to produce a prototype. The ability to design a product and basically overnight print it to have it ready the other day without casting a mold or waiting for a company to produce and ship it is invaluable in research and development situations. However, the 3D printers' do not only offer benefits for prototype and R&D productions. The way 3D printers operate provides a cost per piece graph that is almost constant for each piece assuming the 3D printer buying cost can be

neglected (which can be if one is to produce a lot of different parts.)

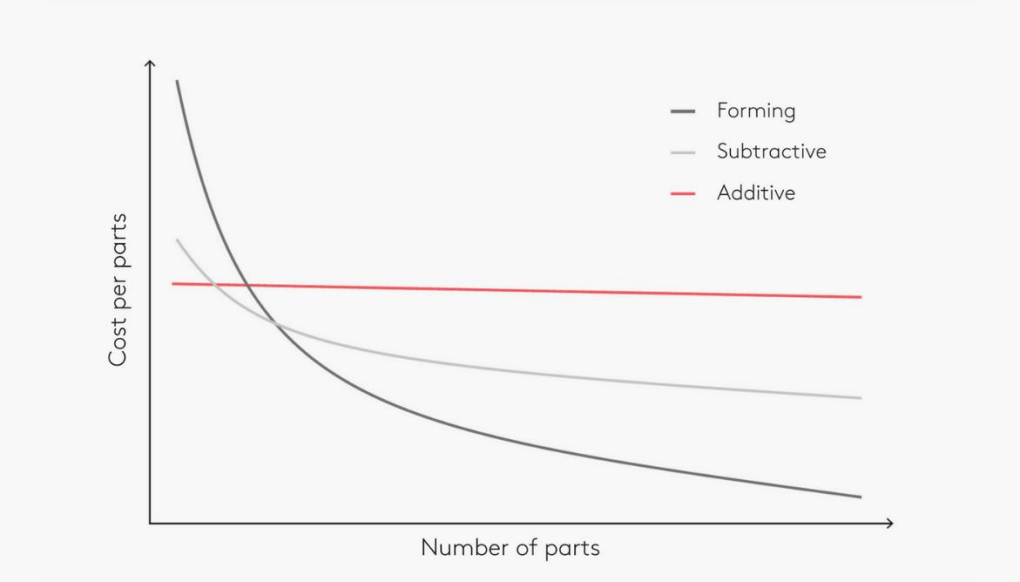

https://bitfab.io/blog/additive-manufacturing/

As one can see in the graph above additive manufacturing can be the cheapest option to produce parts under a certain number.

Types of 3D printing:

There are 3 main types of 3D printers categorized on their working principles that are used today. These are: SLS, SLA/DLP and FDM/FFF.

SLS (Selective Laser Sintering):

This type of Additive manufacturing uses a laser and a powdered material bed. The laser selectively melts the powdered material in the bed and creates one layer of material. This process repeats for each layer. This type of additive manufacturing is especially used to additively build metal parts.

SLA or DLP (Stereolithography or Digital Light Processing)

These two 3d printing technologies in principal are very close to each other. Both use a pool of liquid resin that is selectively cured by light. The difference between SLA and DLP is that

DLP uses an additional light source like an LCD display. This makes the printing speed way faster than SLA which uses a laser which is why it takes a longer time to print a product.

FDM or FFF (Fused Deposition Modeling or Fused Filament Fabrication):

Maybe the most commonly known 3D printing technique is FFF which is the same as FDM that is a brand name. FFF technology uses a filament that is melted through a nozzle and freezes where it is printed. This technology is the most widespread type of 3D printers mainly because of its affordability. Two of the most commonly used filament types are ABS and PLA.

https://penandplastic.com/3d-printer-types/

Though the materials used for FFF are durable and can be used for high-performance tasks, the action of 3D printing introduces a lot of potential for flaws in the structures themselves. This combined with the obvious fiber composite like print direction that exists in FFF the material properties could potentially highly differ from parts produced using molding processes.

In this thesis I will explore the different material properties of 3D printed structures dependent on their base material and their print direction. Using these properties, I will design a simple wind and analyze it using CFD Fluent and Static Structural analysis of the Ansys program.

Material Properties

One of the aims of this thesis is to explore how and if 3D printing changes the properties of the used material. The material properties for FFF may differ with print orientation, layer height, extruder temperature and print speed, among others. The static structural analysis conducted will only consider the mechanical differences caused by print orientation. Since we are using FFF material selection will be generic brand ABS and PLA.

The effects of Layer height:

Layer height is one of the parameters that can be changed to achieve better resolution or higher printing speed. The increase in layer height results in a lower resolution of the printed part but offers a lower print time.

The mechanical changes due to layer height are described **Highertensile strengthis noted at the lower layer height dueto larger bonding area between layer interfaces. rajpurohit2018**

The effects of Extruder Temperature:

The extruder temperature can affect the time the printed polymer spends in glass transition state. This can increase the bonding between layers and roads printed. The affect the extruder temperature has is described by **abbott2018 "Extruder temperature played a more minor role than print speed, but increasing the temperature led to increased tensile strength and contact length."**

The effects of print speed:

The print speed is one of the most important parameters considered before any print, since the yield of a single printing batch greatly depends on the printing speed. While everyone using a 3D printer would want to print as fast as possible, the increase in print speed unfortunately decreases the strength of the printed parts as mentioned by **abbott2018 "Increasing print speed was found to negatively affect the tensile strength and contact length for both print orientations."**

The effect of Print Orientation:

The print orientation of 3D printed parts can be compared to unidirectional fiber composite parts. FFF 3D printed parts have a filament printing direction for each layer which then bonds with nearby layers and roads. This can be compared to fibers which are bonded together by the matrix in between them. The difference though would be that there is not such a high property difference in the material like fiber and matrix have.

Printing orientation not only changes the tensile strength of parts, it also changes the isotropic properties of the polymer since the print direction and transverse direction should have different properties.

Tensile tests done by Y. Song, Y. Li, W. Song, K. Yee, K.-Y. Lee and V.L. Tagarielli on the effect of print direction on 3Dprinted PLA. Results are shown in figure X.X

Since the analysis is going to be conducted as static structural rather than dynamic, the lower strain rate test results are going to be taken into consideration.

According to the test results in figure X.X it can be clearly seen that in terms of yield strength 45-degree raster orientation provides the best results for 3D printed PLA. However surprising is that all three print orientations have resulted in a more durable material compared to the molded version, in terms of tensile properties.

Tests conducted by R. Hernandez, D. Slaughter, D. Whaley, J. Tate, and B. Asiabanpour on 3D printed ABS 430 in different directions have provided the results that can be seen in figure X.X

These results, although they do not include yield strength, clearly show the superiority of PLA over ABS430 both in terms of tensile strength and modulus.

The yield strength not provided in figure **X.X** can however be estimated from figure **X.X. These estimates are, 9.5 MPa for 90-degree Z, 9.7 MPa for 45-degree Z, 9MPa for 45-degree XY, and 9.5 MPa for 0-degree XY. 90-degree XY has not been considered since it has a nonlinear graph.**

From these mechanical property results the ones to consider are:

For PLA, 0-45-90-degree, and molded properties for $1.25\text{x}10^{-5}$ stain rate.

For ABS 430, 0 and 45-degree XY. Since the Z directions are very brittle as seen in Figure **X.X** which is an unwanted property for aircrafts the Z direction materials were not considered. The 90-degree XY direction has been dismissed since the stress-strain graph is nonlinear.

Wing Design

For this project's wing design a similar wing study was conducted. The aim of this study was to find a UAV that has a wing structure that is self-sustaining through 3D printed parts only. No carbon fiber rods used as spar or any other external help for the structural integrity of the wing.

One such plane was found to be the “Eclipson model T”. The Eclipson Model T has a wingspan of 116 cm, aspect ratio of 6.5 and uses a NACA 4415 profile. The Eclipson Model T also has a stall speed for PLA printed structure of 29Km/h or around 8m/s. https://www.eclipson-airplanes.com/modelt

Additional research was done to determine the spar structure to be considered. According to A F HughesD C IlesA S Malik “the torsional stiffness of hollow sections is much greater than that of open sections of comparable size”.

So instead of using an I beam which is the most commonly used beam structure, a rectangular structure should be considered since if the horizontal and vertical walls add up to the same thickness there should not be a bending difference if the beam has an open or closed section. Beams with the highest torsional resistance are circular hollow beams.

Initial wing design

Initially the wing was supposed to consist of an outer skin supported with one spar located at the ¼ cord line. This design was produced and analized under a 0 degree angle of attack and 25m/s airspeed. The result can be seen in Figure **X.X**

As can be seen the lower side skin of the wing is pushed inwards. A clear sign of a lack of structural integrity at the back half of the wing. The solution would be to locate a second spar at the ¾ cord line to support the wing skin around there. The final wing design can be seen in figure **X.X** . 3 spar structures were considered, silindrical, rectangular and parallelogram . The parallelogram was considered since the rectangular spar structure was narrow on one side and thich on the other side where the airfoil was wider. So the question arose would there be a positive aspect to having the top and bottom spar edges be parallel to the airfoil.

The final wing sections can be seen in figures, **X.X X.X X.X.**

Analysis

To assess the structural integrity of the different wing structures using the different material properties, the first order of business was to analyze a flow over the wing structure and then export that data to static structurally analyze the response.

Fluent-Cfd analysis

The wing structure was analyzed in a 3d fluent configuration without the wing tips being considered. The wind tunnel structure created was as wide as the wing, so to not allow any flow around the wing tip. This was done to only consider the wing since in real time not only wing tip but also fuselage effect would have to be considered which have both been neglected for this project. In figure **X.X** the wing structure can be seen alone, and in figure **X.X** the wing structure can be seen with the wind tunnel volume together.

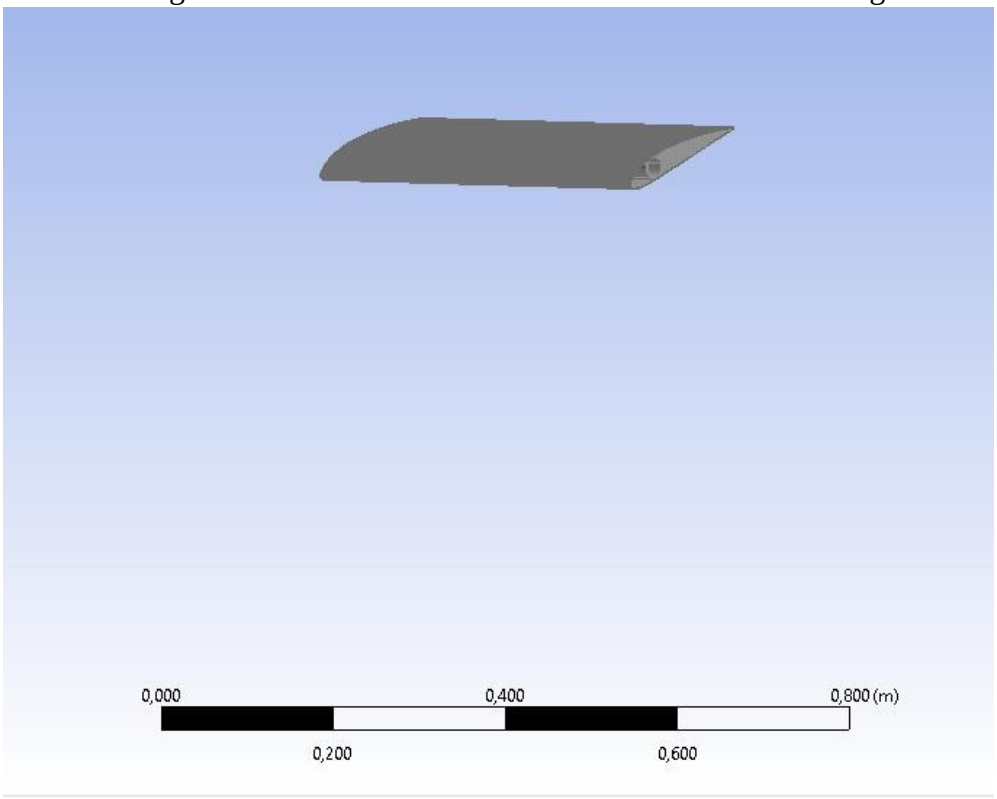

Figure

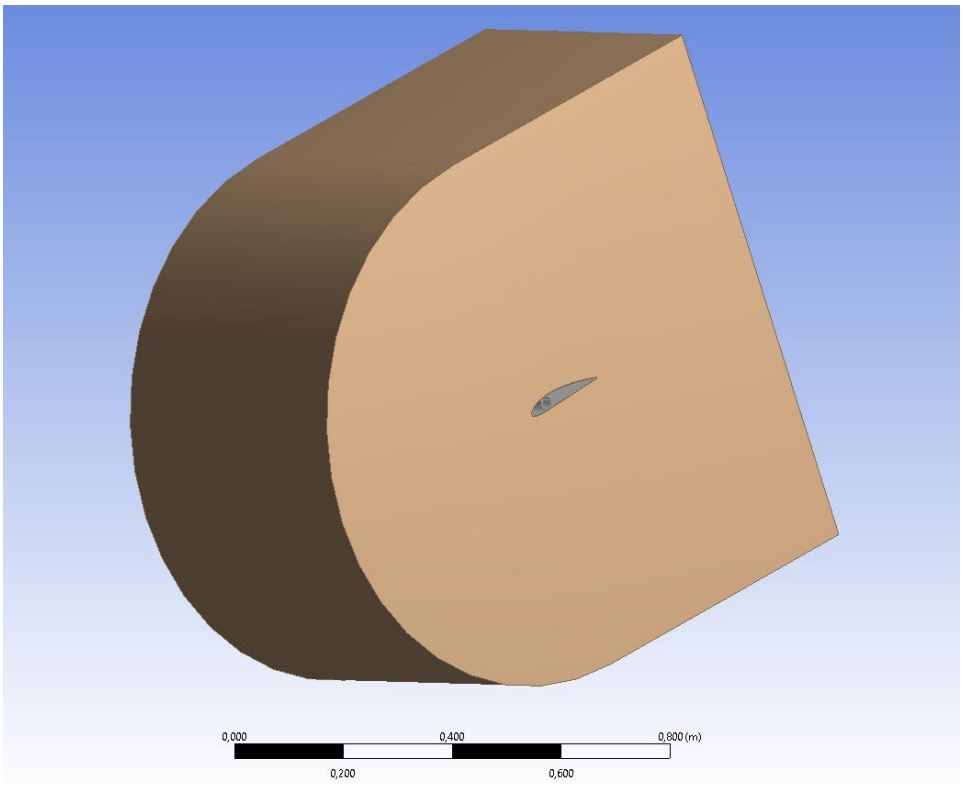

Figure

Meshing

The structure was meshed with a 12.5mm element size that shrank down to 2.5 mm at the airfoil surface. The total node count added up to 350235 with a total element count of 331980.

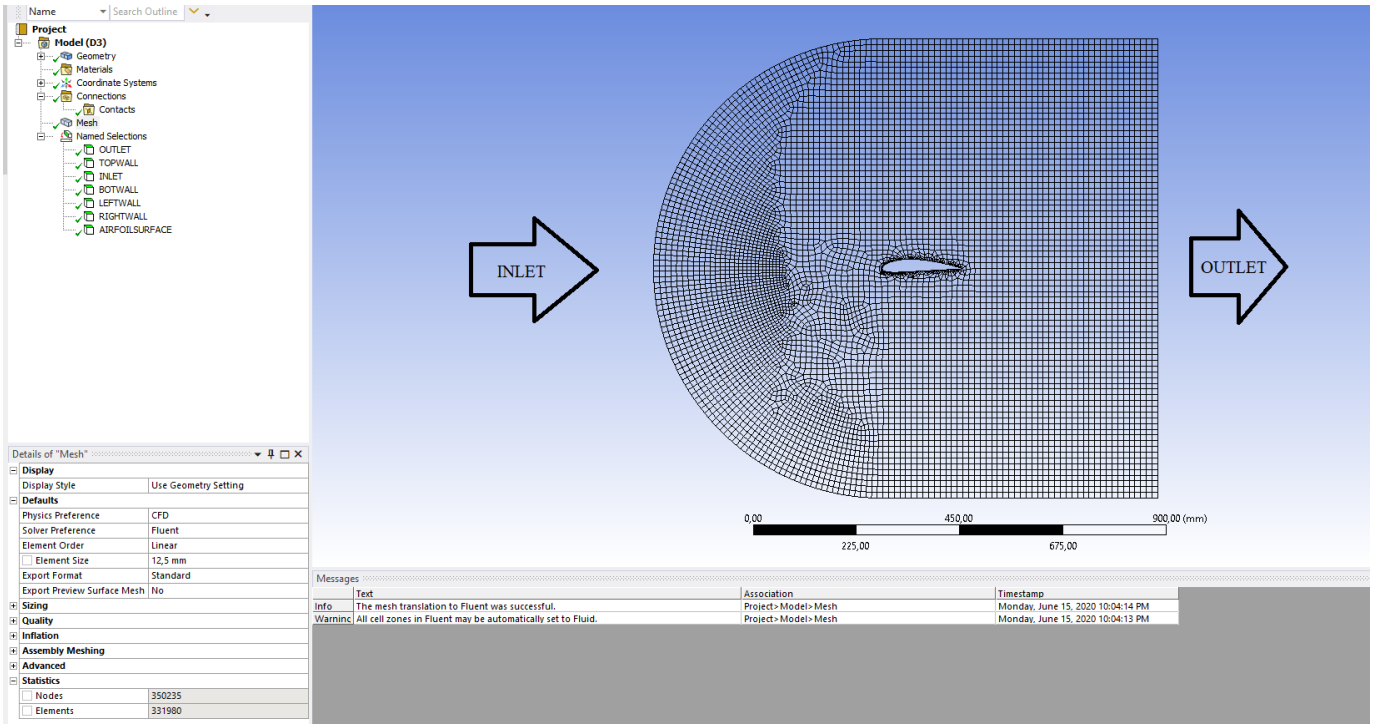

Fluent Results

The results of the Fluent analysis under a 25m/s inlet velocity can be seen in figure **X.X**.

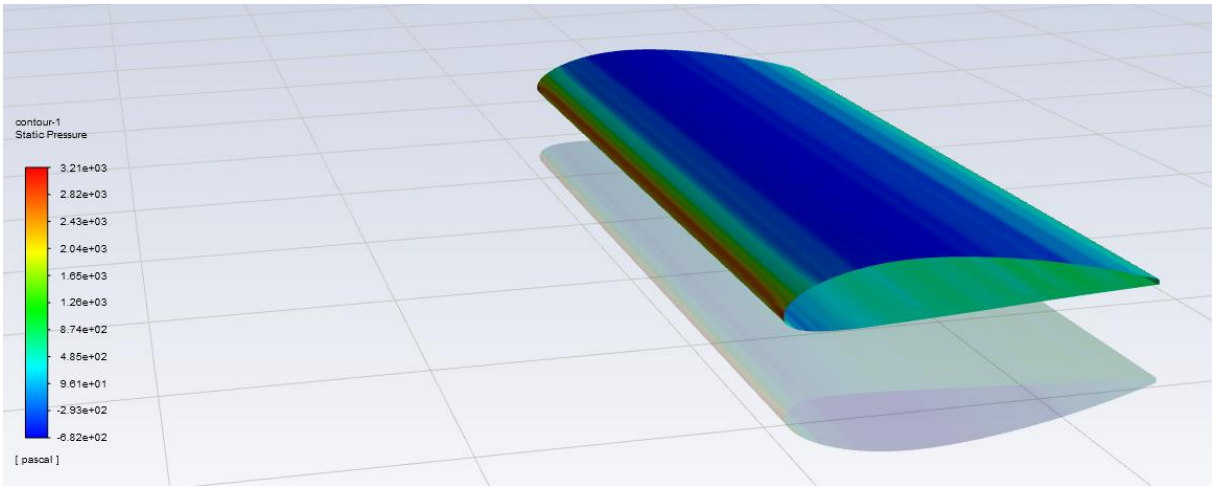

figure

The results will be distributed onto the wing in a static structural analysis.

Static Structural Analysis

The static structural analysis has been conducted to determine the structural response under the different wing spar geometries and the different material configurations.

Meshing (finite element modeling)

Since the structural analysis will be repeated many times the mesh count has to be optimized. To determine the mesh independency 2 mesh configurations were analyzed to compare the results. If the results were to differ less than 1% the lower mesh count will be used.

High Nod Version

The upper limit for the mesh was not chosen as much as it was a physical limitation. The upper mesh limit was the mesh count that the computer used could support due to limited RAM space. The mesh generated had a nod count of 1153103 and an element count of 645368 as can be seen in figure **X.X**.

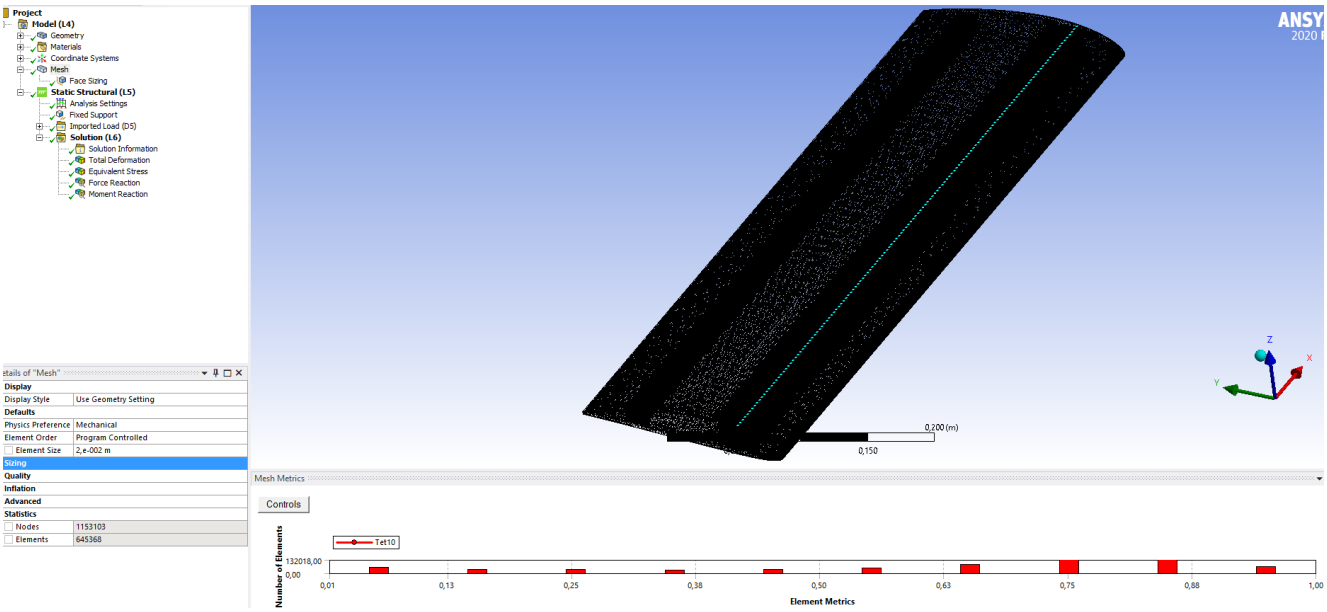

Figure

A static structural analysis was done on this generated mesh structure using the fluent results. The run time was almost 20 min with a memory usage of 6.7 GB as can be seen in figure **X.X**.

Information	
Status	Done
MAPDL Elapsed Time	19 m 49 s
MAPDL Memory Used	6,707 GB
MAPDL Result File Size	415,94 MB

The results of the High mesh count analysis in terms of maximum equivalent stress (von Mises) was 6.55 MPa figure **X.X**.

Results	
Minimum	323,34 Pa
Maximum	6,55e+006 Pa
Average	1,0821e+006 Pa

Figure

Low mesh count

The lower limit was chosen by changing the element size. To be twice the size for the outer surface and 5 times the size for the spar structures. The final mesh generated had a nod count of 165609 and an element count of 85385. This can be seen in figure **X.X**.

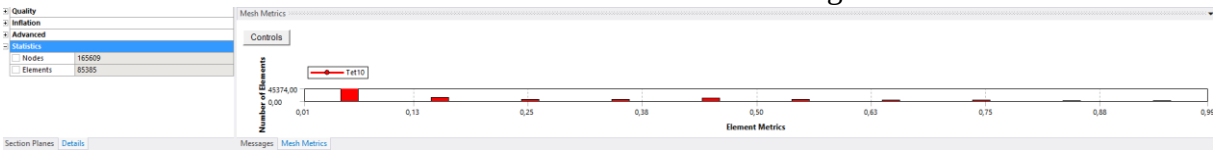

Figure

A static structural analysis was done on this generated mesh structure using the fluent results. The run time was just 1 min with a memory usage of 3,125GB as can be seen in figure **X.X**.

Information	
Status	Done
MAPDL Elapsed Time	1 m 2 s
MAPDL Memory Used	3,125 GB
MAPDL Result File Size	61,313 MB

Figure

The run time has been lowered significantly even though the memory usage just halved.

The results of the Low mesh count analysis in terms of maximum equivalent stress (von mises) was 6.5244 MPa figure **X.X**.

Results	
Minimum	1329,1 Pa
Maximum	6,5244e+006 Pa
Average	1,2135e+006 Pa

Figure

If the results are compared to show the error stemming from the low mesh count:

$$\frac{6{,}55 - 6{,}5244}{6{,}55} = 0{,}003908 = 0{,}3908\%\ error$$

Since the error is below 1% this lower mesh count can be used. There is no real reason to go for a lower mesh count since the run time is already very low at 1 minute.

Cylindrical spar results

The first structure that was analyzed was the cylindrical sparred wing structure. The stress results were the same for all material selections. The equivalent stress distribution can be seen in figures **X.X** and **X.X**.

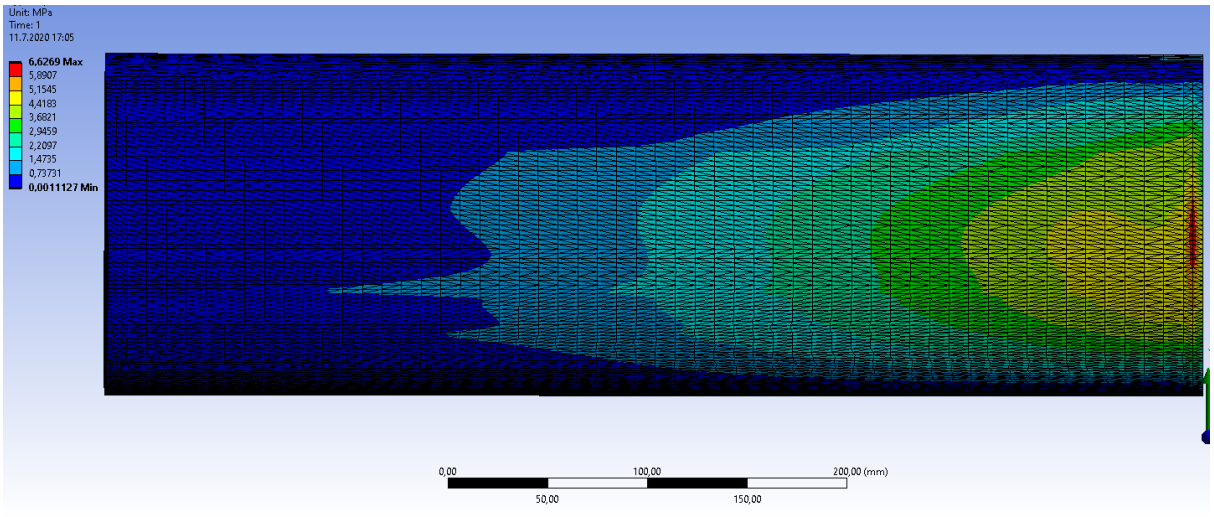

Figure

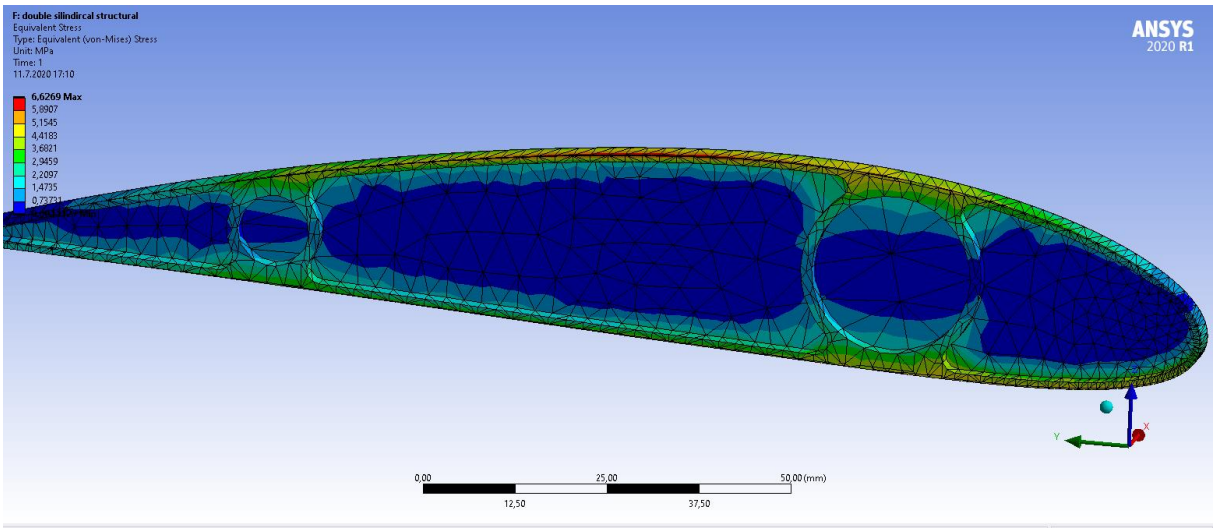

Figure

The maximum von mises equivalent stress acting upon the wing is located on the top middle skin of the wing on the root section.

Although the total distribution differs by material type the distribution of lower deformation to higher deformation is similar across all material types and can be seen in figure **X.X**.

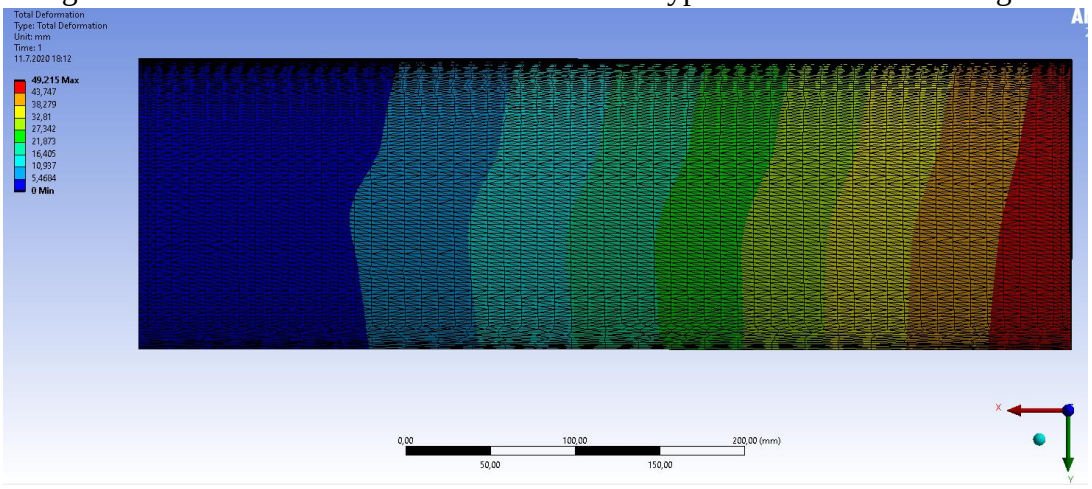

Figure

The total deformation distribution across different material types analyzed has been compiled into table **X.X**.

Cylindrical Spar	Von Mises Eq. Stress (Mpa)	Wing Tip Total Deformation (mm)	
ABS 0 Degree	6.6269	51.586	
ABS 45 Degree	6.6269	49.215	
PLA 0 Degree	6.6269	9.7351	
PLA 45 Degree	6.6269	9.0804	
PLA 90 Degree	6.6269	8.6745	
PLA Molded	6.6269	9.7046	

Table

The results clearly show the superiority of PLA over ABS in all print directions. The least deformation has been shown to be the 90-degree raster-oriented PLA. On the other hand, the 0-degree oriented PLA has been shown to be the worst orientation among printed PLA and even worse than molded PLA. However, the inter-material result differences are very close having a 12% deformation increase between the best and worst PLA orientation. The Abs material though, has a significant disadvantage in terms of deformation at least in bending and wing design applications.

Rectangular Wing Analysis

The second structure that was analyzed was the rectangular sparred wing structure. The stress results were the same for all material selections. The equivalent stress distribution can be seen in figures **X.X** and **X.X**.

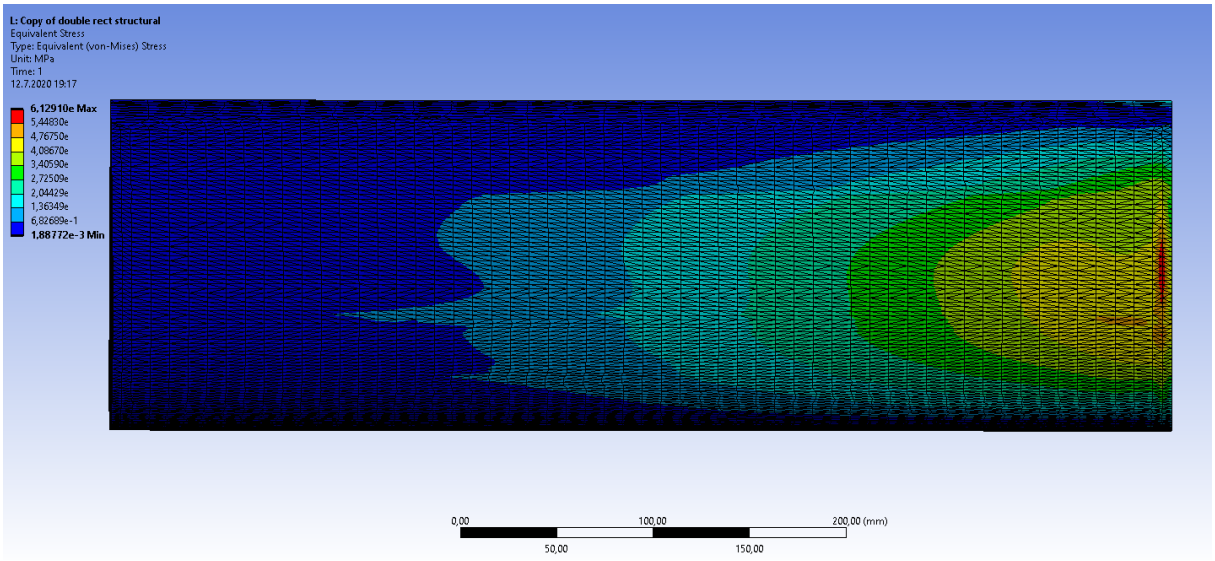

Figure

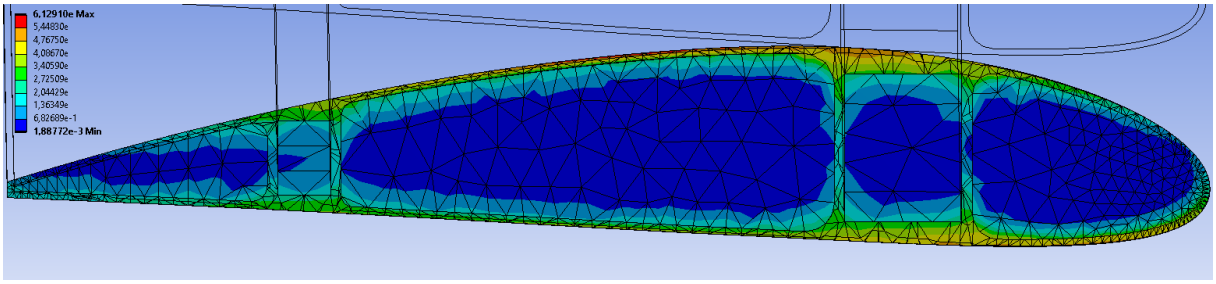

Figure

The maximum von mises equivalent stress acting upon the wing is located on the top middle skin of the wing on the root section just as on the cylindrical sparred wing structure.

Although the total distribution differs by material type the distribution of lower deformation to higher deformation is similar across all material types and can be seen in figure **X.X**.

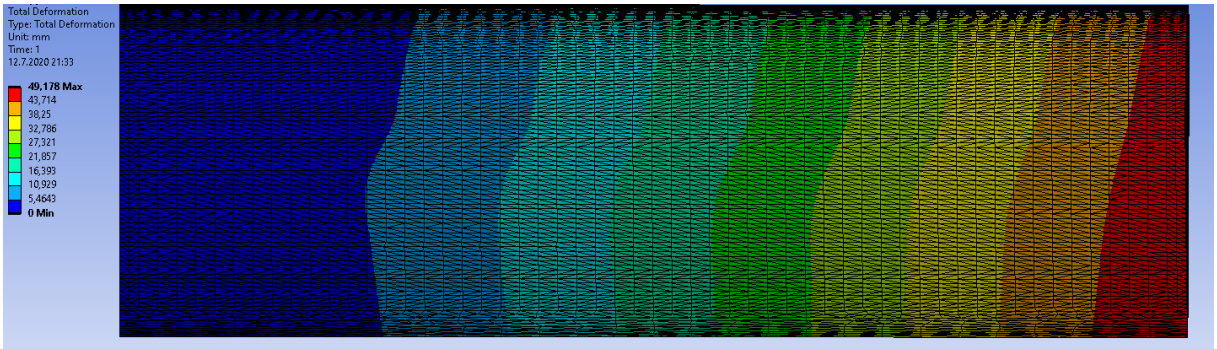

Figure

The total deformation distribution across different material types analyzed has been compiled into table **X.X**.

Rectangular Spar	Von Mises Eq. Stress (Mpa)	Total Deformation
ABS 0 Degree	6.1291	49.178
ABS 45 Degree	6.1291	46.918
PLA 0 Degree	6.1291	9.2807
PLA 45 Degree	6.1291	8.6565
PLA 90 Degree	6.1291	8.2696
PLA Molded	6.1291	9.2517

Table

As in the results for the cylindrical wing, these results also show the clear supremacy of PLA over ABS. Since the material properties are the same as the ones used in the cylindrical sparred wing, the differences according to material are the same as well. However, the results of the rectangular sparred wing show that for total deformation as well as Equivalent stress rectangular spars structurally better suited than cylindrical spars. Having the same volume and cross-sectional area, the rectangular spars gave the wing a sounder structure decreasing the von Mises equivalent stress by 7.5% compared to the cylindrical sparred wing.

Parallelogram sparred wing

The final structure that was analyzed was the parallelogram sparred wing structure. The stress results were the same for all material selections. The equivalent stress distribution can be seen in figures **X.X** and **X.X**.

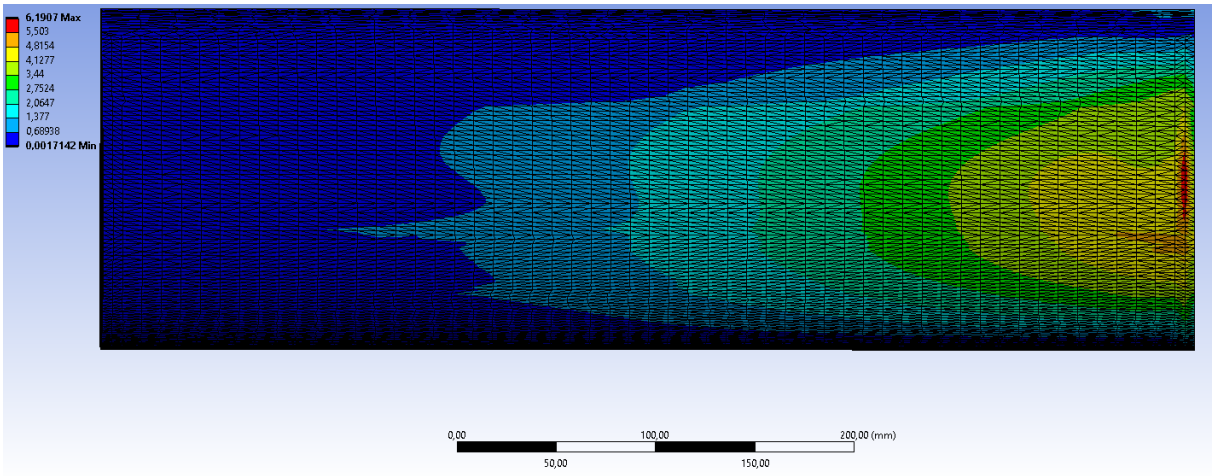

Figure

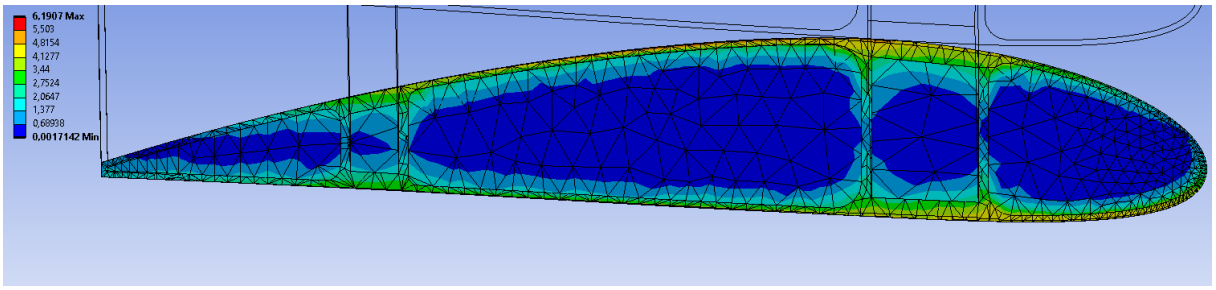

Figure

The maximum von mises equivalent stress acting upon the wing is located on the top middle skin of the wing on the root section just as on the cylindrical sparred and rectangular sparred wing structures.

Although the total distribution differs by material type the distribution of lower deformation to higher deformation is similar across all material types and can be seen in figure **X.X**.

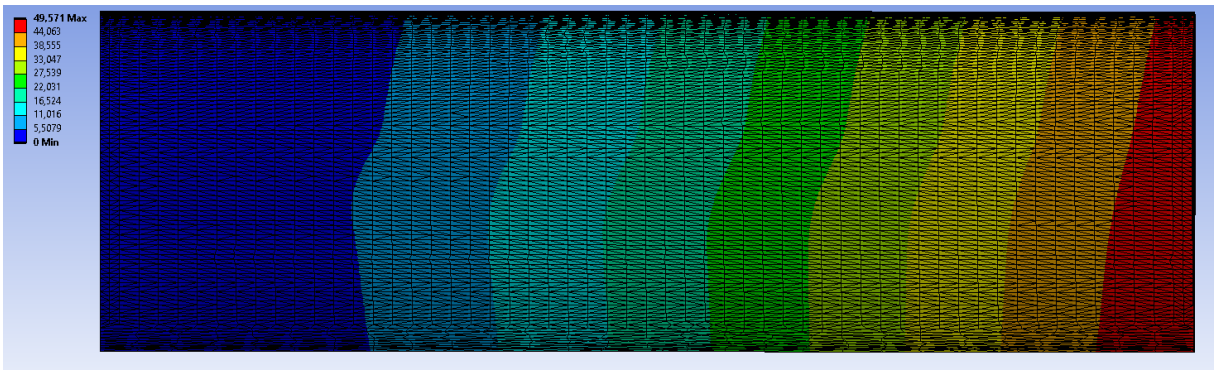

Figure

The total deformation distribution across different material types analyzed has been compiled into table **X.X**.

Parallel Spar	Von Mises Eq. Stress (Mpa)	Wing Tip Total Deformation (mm)	
ABS 0 Degree	6.1907	49.571	
ABS 45 Degree	6.1907	47.293	
PLA 0 Degree	6.1907	9.3547	
PLA 45 Degree	6.1907	8.7256	
PLA 90 Degree	6.1907	8.3357	
PLA Molded	6.1907	9.3255	

Table

The experimental spar form proved to be worse than the rectangular sparred wing structure. Having the same crosssectional area and total volume as the rectangular sparred wing the parallelogram sparred wing performed worse by 1% in terms of maximum equivalent Von Mises stress. This 1% worsening of performance could be considered in the margin of error

since the mesh independency alone had a 0.39% error margin and 1% error margin was accepted.

Conclusion

In conclusion, among the three spar structures analyzed the rectangular spars performed better than their counter parts although just slightly better than the parallelogram spar. The cylindrical spar has performed the worst which was expected since the moment of inertia of a ring is less for the same cross-sectional area as a hollow rectangle. Among the materials analyzed the best performance was given by 90-degree raster-oriented PLA, followed by 45-degree and molded respectively. Abs performed the worst by a lot due to its chemical properties rather than the printing effects. Following the unidirectional fiber composite logic, it would have been expected that the 0-degree raster oriented material should perform the best since there is no bonding or potential flaws in the tensile direction which proved not to be the case. Molded on the other hand should be expected to perform even better than any 3D printed material since the molding process minimizes the flaw potential in the material. This turned out to not be the case. Molded, only outperformed the 0-degree printed material.